

THERMAL STUDIES OF BIS SALICYLIDENE ADIPIC DIHYDRAZONE DERIVATIVES AND THEIR COMPLEXES WITH DIVALENT IONS OF Mn, Co, Ni, Cu AND Zn

R. M. Issa*, S. A. Amer, I. A. Mansour and A. I. Abdel-Monsef

Department of Chemistry, Faculty of Science, Tanta University, Tanta, Egypt

The thermal stabilities of bis salicylidene adipic dihydrazone derivatives and their complexes with divalent Mn, Co, Ni, Cu and Zn were studied and discussed in terms of structure and type of metal ions. TG curves display mostly four steps of thermal decomposition. The first step is due to dehydration, then the elimination of the acetate anions followed by the decomposition of the ligand in two interacting steps. The activation energies E_a were evaluated and discussed in accordance with the structure of the complexes which have been previously characterized by elemental analysis and IR spectra. It was found that the activation energies of the complexes based on bis salicylidene adipic dihydrazone were higher than those of the dihydroxy derivative.

Keywords: activation energy, dihydrazones, metal complexes, thermal analysis

Introduction

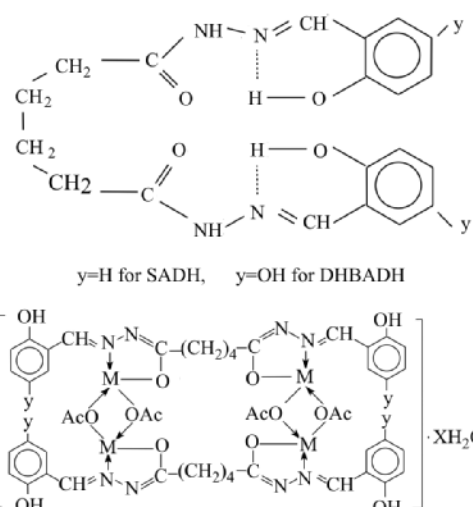
Schiff bases and their metal complexes are known to be biologically important [1–3]. DTA and TG were used to study the modes of thermal decompositions as well as the composition of some divalent copper, cobalt and nickel complexes of Schiff bases [4, 5]. The studies also included the determination of thermokinetic parameters [6]. The stoichiometry of thermal decomposition and the relationship between the thermal parameters of the complexes were studied by some authors [7]. The thermal behavior of synthetic pyroaurite [8], dissociation process for clathrates [9], thermal analysis for fly ash based zeolites [10] and DTA/TG/MS of polymethyl methacrylate were studied [11]. The thermal analysis study of different azo and azomethine complexes has been the subject of intense research in our laboratory for several years [12]. Accordingly, in this work we aimed to study the thermal analysis (TG and DTA) as well as the kinetic parameters of decomposition of some complexes prepared from Schiff bases of adipic dihydrazide.

Experimental

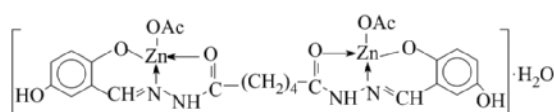
The preparation details and structure of the ligands and their metal complexes are reported elsewhere by the present authors [13].

The differential thermal analysis (DTA) and thermogravimetric analysis (TG) were carried out on a Shimadzu DT-30 and TGA-50 thermal analyzers

within the temperature range 20–800°C at a rate of 20°C min⁻¹, using purified nitrogen gas in the surrounding atmosphere [14]. The ligands and complexes under investigation were found to have the following structures:



where $M=\text{Mn(II)}, \text{Co(II)}, \text{Ni(II)}, \text{Zn(II)}, X=1, y=\text{H}; M=\text{Cu(II)}, X=4, y=\text{H}; M=\text{Mn(II)}, \text{Co(II)}, \text{Cu(II)}, X=1, y=\text{OH}; M=\text{Ni(II)}, X=3, y=\text{OH}$

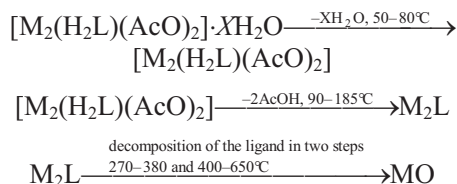


* Author for correspondence: Amonsef5000@yahoo.com

Results and discussion

TG and DTA study

The results of thermal analysis of the prepared ligands SADH and DHBADH (Tables 1 and 2) show a weak exothermic peak without mass loss at 40–50°C due to the cleavage of hydrogen bond and rearrangement of the ligands. The ligands show thermal stability behavior up to 320 and 285°C for SADH and DHBADH, respectively. The sharp endothermic peak with mass loss of 55 and 58% is due to melting with cleavage at the two (C=N) and loss of the two aldehyde groups followed by further decomposition are expected. The results of the thermogravimetric analysis of the metal complexes under study (Fig. 1; Tables 1 and 2) show the loss of their hydration water below 100°C. The anhydrous complexes lose two acetic acid molecules within the temperature range 90–185°C and then display the decomposition of the organic ligand in two strongly interacting steps within the temperature range 270–650°C leading to formation of the metal oxides. The metal contents were calculated from the mass of the solid residue and found to be in good agreement with the results of the elemental analysis within satisfactory experimental errors. The reactions representing the three steps of thermal decomposition of the metal complexes can be given as follows:



The first step with TG step in the range 50–80°C is related to the volatilization of the lattice water molecules. This finds support from the disappearance of the bands due to the various modes of vibration of the water molecules ($\nu_{\text{H}_2\text{O}}$ at 3400 cm^{-1} , in plane deformation $\delta_{\text{H}_2\text{O}}$ at 1350 cm^{-1} and out of plane deformation $\gamma_{\text{H}_2\text{O}}$ at 975 cm^{-1}) in the spectra of the complex I heated at 90°C for 3 h in a drying oven as shown in Fig. 2. For most complexes an endothermic mass loss was observed following the first step, which corresponds to the loss of two acetic acid molecules. The IR spectra of 185°C-heated metal complexes depict the disappearance of the acetate group frequencies situated at 1470–1435 and 1386–1326 cm^{-1} assigned to ν antisymmetric and ν symmetric bidentate acetate, respectively [15–17]. In the third step of decomposition, the organic ligand is lost within the temperature range 270–650°C, with the formation of the corresponding metal oxides. On the basis of the above results one can conclude the following:

- lattice water is removed from the prepared homobinuclear complexes at 50–80°C
- coordinated acetate ions are removed within the range 90–185°C and
- thermal stability of the complexes of SADH are higher than that of DHBADH

Accordingly, the thermal decomposition course of the complexes proceeds as formulated in Scheme 1.

The order (n) and the energy of activation (E^*) of the decomposition steps were determined using the Coats–Redfern equation [18, 19] in the form:

$$\ln[1-(1-\alpha)^{1-n}/(1-n)T^2] = M/T + B \text{ for } n \neq 1 \quad (1)$$

$$\ln[-\ln(1-\alpha)/T^2] = M/T + B \text{ for } n = 1 \quad (2)$$

where $M = -E^*/R$, $B = \ln AR/\Phi E^*$; R =gas constant, A =pre-exponential factor and Φ =heating rate ($20^\circ\text{C min}^{-1}$).

The correlation factor, r , is computed using the least squares method for Eqs (1) and (2). Linear

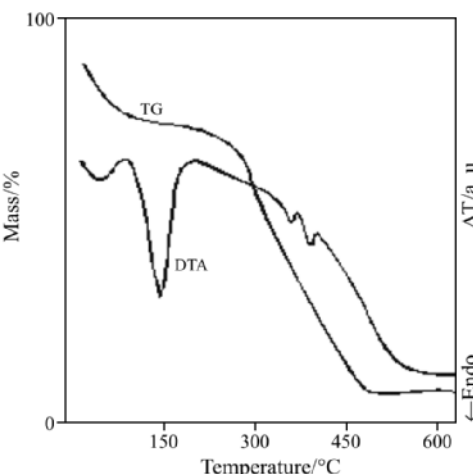


Fig. 1 DTA and TG curves of complex **VIII**

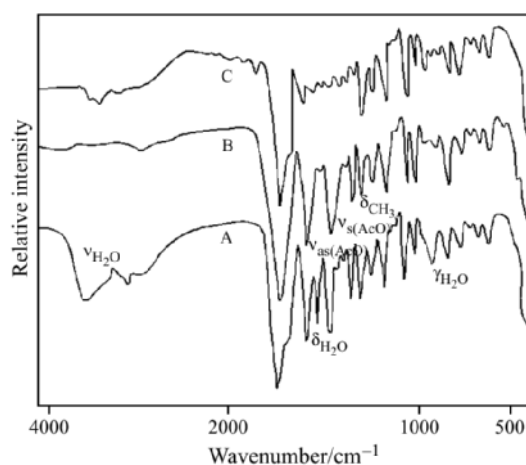


Fig. 2 IR spectra of complex I; A – original complex, B – after heating to 90°C and C – after heating to 160°C

Table 1 Thermal analysis data of salicylidene adipic dihydrazone (SADH) and its divalent metal complexes

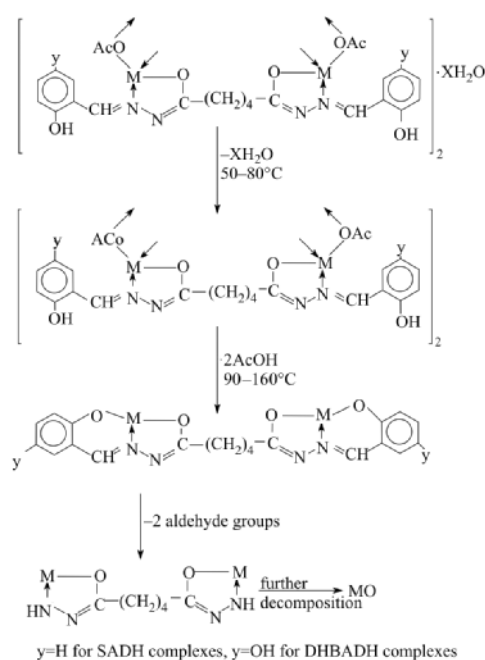
Complex	DTA peaks			TG steps			Assignment
	temperature	peak	temperature range	calcd.	found	mass loss/%	
SADH (H_4L^1)	40–50 320 330, 340	exo endo (sh) endo (w)	300–320 320–380 380–600	55.5 70.1	— 71.1	55.0 71.1	cleavage of hydrogen bond and rearrangement cleavage of $2\text{C}=\text{N}$ and loss of 2 aldehyde groups ($\text{C}_{12}\text{H}_{10}\text{O}_2$) loss of nitrogen as NO_2 further decomposition
$[\text{Mn}_2(\text{H}_2\text{L}^1)\text{X}_2]_2\text{H}_2\text{O}$ (I)	50 350	exo (w) endo (w)	50–70 140–160 350–370 400–650	2.95 18.8 29.0 21.7	3.55 19.2 28.5 20.5	loss of one molecule of lattice H_2O and rearrangement loss of two acetic acid molecules melting with decomposition further decomposition and formation of MnO_2 as stable form	
$[\text{Co}_2(\text{H}_2\text{L}^1)\text{X}_2]_2\text{H}_2\text{O}$ (II)	50–75 340–370	exo (w) endo (w) endo (w)	60–80 100–140 340–500 560–650	2.88 18.7 42.7 30.2	3.25 17.9 42.0 31.0	loss of one molecule of lattice H_2O and rearrangement loss of two acetic acid molecules melting with decomposition, cleavage of $2\text{C}=\text{N}$ and loss of two aldehyde groups ($\text{C}_{12}\text{H}_{10}\text{O}_2$) further decomposition and formation of CoO as stable form	
$[\text{Ni}_2(\text{H}_2\text{L}^1)\text{X}_2]_2\text{H}_2\text{O}$ (III)	70 400	exo (w) endo (w) endo (sh)	50–70 90–160 390–520 600–650	2.87 18.8 41.2 22.9	3.52 19.4 42.0 21.8	loss of one molecule of H_2O and rearrangement loss of two acetic acid molecules melting with decomposition, cleavage of $2\text{C}=\text{N}$ and loss of two aldehyde groups ($\text{C}_{12}\text{H}_{10}\text{O}_2$) further decomposition and formation of NiO as stable form	
$[\text{Cu}_2(\text{H}_2\text{L}^1)\text{X}_2]_2\text{H}_2\text{O}$ (IV)	50–90 275–310 325, 360	exo (w) endo (w) exo (sh) exo (w)	50–70 80–140 270–310 350–460	5.76 16.2 28.1 28.4	6.21 17.8 31.5 28.0	loss of four molecules of H_2O and rearrangement loss of two acetic acid molecules melting with decomposition, cleavage of $2\text{C}=\text{N}$ and loss of two aldehyde groups ($\text{C}_{12}\text{H}_{10}\text{O}_2$) further decomposition and formation of CuO as stable form	
$[\text{Zn}_2(\text{H}_2\text{L}^1)\text{X}_2]_2\text{H}_2\text{O}$ (V)	70–80 320 350, 400 430	exo (w) endo (w) exo (sh) exo (w)	70–80 90–160 320–410 450	2.87 18.8 40.3 30.7	3.6 20.0 40.0 30.0	loss of one molecule of H_2O and rearrangement loss of two acetic acid molecules melting with decomposition, cleavage of $2\text{C}=\text{N}$ and loss of two aldehyde groups ($\text{C}_{12}\text{H}_{10}\text{O}_2$) further decomposition and formation of ZnO as stable form	

$\lambda = \text{Ac}_2\text{O}$; w=weak and sh=sharp peaks

Table 2 Thermal analysis data of dihydroxy bezylidene adipic dihydrazone (DHBADH) and its metal complexes

Complex	DTA peaks			TG steps		
	temperature	peak	temperature range	mass loss/% calcd.	mass loss/% found	Assignment
DHBADH (H_4L^2)	40–50	exo (w)	—	—	—	cleavage of hydrogen bond and rearrangement
	285	endo (sh)	280–330	29.5	27.5	melting with successive cleavage of $2\text{C}=\text{N}$ and loss of 2 aldehyde groups ($\text{C}_{12}\text{H}_{10}\text{O}_2$)
	330	exo (sh)	330–560	58.9	58.0	further decomposition
$[\text{Mn}_2(\text{H}_2\text{L}^2)\text{X}_2]_2\cdot\text{H}_2\text{O}$ (VII)	350–380	exo (w)	560–700			
	70	exo (w)	60–80	2.77	3.3	loss of one molecule of H_2O and rearrangement
		endo (br)	120–170	18.2	19.0	loss of two acetic acid molecules
$[\text{Co}_2(\text{H}_2\text{L}^2)\text{X}_2]_2\cdot\text{H}_2\text{O}$ (VII)	110–180	exo (br)	290–340	29.3	30.5	melting with decomposition, cleavage of $2\text{C}=\text{N}$ and loss of 2 aldehyde groups ($\text{C}_{12}\text{H}_{10}\text{O}_2$)
	300	endo (w)	400–600	28.1	29.2	further decomposition and formation of MnO_2 as stable form
	370, 400					
$[\text{Ni}_2(\text{H}_2\text{L}^2)\text{X}_2]_2\cdot 3\text{H}_2\text{O}$ (VIII)	70	exo (w)	50–80	2.7	3.4	loss of one molecule of H_2O
	100–170	endo (br)	120–180	17.7	18.4	loss of two acetic acid molecules
	250–300	endo (br)	300–400	27.9	28.5	melting with cleavage of $2\text{C}=\text{N}$ and loss of two aldehyde groups ($\text{C}_{12}\text{H}_{10}\text{O}_2$)
$[\text{Cu}_2(\text{H}_2\text{L}^2)\text{X}_2]_2\cdot\text{H}_2\text{O}$ (IX)	350–420	endo (w)	450	23.1	24.0	further decomposition and formation of CoO as stable form
	70	exo (sh)	55–80	7.7	8.4	loss of three molecules of H_2O and rearrangement
	115–170	endo (br)	130–185	16.8	17.5	loss of two acetic acid molecules
$[\text{Zn}_2(\text{H}_2\text{L}^2)\text{X}_2]_2\cdot\text{H}_2\text{O}$ (X)	350, 380	endo (w)	350–400	26.5	25.9	melting with cleavage of $2\text{C}=\text{N}$ and loss of two aldehyde groups ($\text{C}_{12}\text{H}_{10}\text{O}_2$)
			550–660	21.4	19.9	further decomposition and formation of NiO as stable form
$[\text{Cu}_2(\text{H}_2\text{L}^2)\text{X}_2]_2\cdot\text{H}_2\text{O}$ (IX)	50–70	exo (w)	50–70	2.6	3.2	loss of one molecule of H_2O
	90–160	endo (br)	110–170	17.5	18.1	loss of two acetic acid molecules
	270	endo (w)	270–350	27.5	28.4	melting with cleavage of $2\text{C}=\text{N}$ and loss of two aldehyde groups ($\text{C}_{12}\text{H}_{10}\text{O}_2$)
$[\text{Zn}_2(\text{H}_2\text{L}^2)\text{X}_2]_2\cdot\text{H}_2\text{O}$ (X)	320		475–540	15.5	15.7	further decomposition and formation of CuO as stable form
	70	exo (w)	60–75	2.65	3.5	loss of one molecule of H_2O and rearrangement
	100–180	endo (br)	110–180	17.4	18.0	loss of two acetic acid molecules
	220–300	exo (br)	300–360	27.4	27.9	melting with successive cleavage of $2\text{C}=\text{N}$ and loss of two aldehyde groups ($\text{C}_{12}\text{H}_{10}\text{O}_2$)
			460–600	23.9	24.9	further decomposition and formation of ZnO as stable form

$\text{X}=\text{Ac}_2\text{O}$; w=weak; sh=sharp and br=broad peak

**Scheme 1** Thermal decomposition of the comolecules

curves were drawn for values of n ranging from 0–1. The values of n , which gave the best linear plot was chosen as the order parameter for the decomposition stage of interest, and the energy of activation was calculated from its slope.

The other activation kinetic parameters (ΔH^* , ΔS^* , ΔG^*) were computed using the standard equations [5]:

$$\Delta H^* = E^* - RT$$

$$\Delta S^* = R[\ln(Ah/kT)]$$

$$\Delta G^* = \Delta H^* - T\Delta S^*$$

Table 3 Kinetic parameters of decomposition of salicylidene adipic dihydrazone (SADH) and its complexes

Complex	Step	n	r	T/K	Coats–Redfern equation			
					$E^*/\text{kJ mol}^{-1}$	$\Delta H^*/\text{kJ mol}^{-1}$	$\Delta S^*/\text{kJ mol}^{-1}\text{K}^{-1}$	$\Delta G^*/\text{kJ mol}^{-1}$
SADH (H_4L^1)	1 st	0	0.9763	587	11.2	6.39	-0.03	25.25
	2 nd	0	0.9764	775	3.23	-3.21	-0.19	144
[$\text{Mn}_2(\text{H}_2\text{L}^1)\text{X}_2]_2\cdot\text{H}_2\text{O}$ (I)	1 st	0.66	0.9992	310	4.3	1.724	-0.07	25.59
	2 nd	1	0.9887	588	0.3	-4.5	-0.11	58.32
[$\text{Co}_2(\text{H}_2\text{L}^1)\text{X}_2]_2\cdot\text{H}_2\text{O}$ (II)	1 st	0.66	0.9869	333	3.53	0.763	-1.10	367
	2 nd	0	0.9611	703	2.6	-3.24	-1.13	791
[$\text{Ni}_2(\text{H}_2\text{L}^1)\text{X}_2]_2\cdot\text{H}_2\text{O}$ (III)	1 st	1	0.9794	319	0.3	-2.35	-0.10	29.55
	2 nd	0	0.9958	630	6.9	1.66	-0.11	70.9
	3 rd	1	0.9687	742	0.6	-5.5	-0.09	61
[$\text{Cu}_2(\text{H}_2\text{L}^1)\text{X}_2]_2\cdot\text{H}_2\text{O}$ (IV)	1 st	0.66	0.9794	350	2.6	-0.31	-0.15	52.2
	2 nd	0	0.9875	497	5.0	0.86	-0.13	65.5
	3 rd	0.66	0.9844	677	13.9	8.27	-0.01	17.08
[$\text{Zn}_2(\text{H}_2\text{L}^1)\text{X}_2]_2\cdot\text{H}_2\text{O}$ (V)	1 st	0.66	0.9994	313	3.4	0.8	-0.11	35.3
	2 nd	0.66	0.9929	655	6.7	1.26	-0.12	79.85

$X = \text{Ac}_2\text{O}$

where k is Boltzmann's constant and h is the Plank's constant. The necessary values of the temperature were taken from the TG curves at the middle of the step then converted to Kelvin.

The order and the kinetic parameters for thermal decomposition of the ligands and their complexes are listed in Tables 3 and 4. From which it is clear that:

- The negative values of ΔS^* for the dehydration step indicate that the complex is more activated than the reactant and/or the thermal decomposition reaction is slower than normal [20]. This can be explained on the premise that the degradation steps involve simultaneous processes. The first one is the volatilization of the water molecules from the solid complex with positive entropy ΔS^* followed by the formation of a more ordered anhydrous complex with negative ΔS^* value. The determined value is the resultant of the two processes [21]. The second step is the loss of the acetic acid molecules with negative entropy change (ΔS^*). The third step corresponding to the decomposition of the ligand also has a negative entropy change.
- There are no obvious trends in the values of E^* or the activation enthalpy ΔH^* . However, the values of ΔG^* increase for subsequent decomposition steps of a given complex, which means that the second step is slower than the first one [22]. Actually, the values of ΔG^* for the complexes **III** and **IV** increase from first step to second step and then decrease for the third step indicating that for these two complexes the rate of the third step is higher than that of the second. This indicates that in the first step, the free part of the chelated ligand may be subject to partial decomposition then in another step the remainder part is degraded and

Table 4 Kinetic parameters of decomposition of dihydroxy bezylidene adipic dihydrazone (DBHADH) and its complexes

Complex	Step	<i>n</i>	<i>r</i>	T/K	Coats–Redfern equation			
					$E^*/\text{kJ mol}^{-1}$	$\Delta H^*/\text{kJ mol}^{-1}$	$\Delta S^*/\text{kJ mol}^{-1} \text{K}^{-1}$	$\Delta G^*/\text{kJ mol}^{-1}$
DHBADH (H_4L^2)	1 st	0.66	0.9855	565	8.9	4.2	-0.06	38.1
	2 nd	0.66	0.9937	856	6.1	-1.1	-0.15	127
[$\text{Mn}_2(\text{H}_2\text{L}^2)\text{X}_2]_2\cdot\text{H}_2\text{O}$ (VI)	1 st	1	0.9892	328	0.4	2.3	-0.10	30.47
	2 nd	0.66	0.9881	590	6.3	1.4	-0.12	66.3
[$\text{Co}_2(\text{H}_2\text{L}^2)\text{X}_2]_2\cdot\text{H}_2\text{O}$ (VII)	1 st	0.66	0.9974	336	2.9	0.11	-1.12	376
	2 nd	0.66	0.9714	613	6.3	1.21	-1.11	687
[$\text{Ni}_2(\text{H}_2\text{L}^2)\text{X}_2]_2\cdot3\text{H}_2\text{O}$ (VIII)	1 st	1	0.9981	326	0.2	-2.51	-0.11	33.4
	2 nd	0.66	0.9666	706	4.0	-1.87	-0.17	118
[$\text{Cu}_2(\text{H}_2\text{L}^2)\text{X}_2]_2\cdot2\text{H}_2\text{O}$ (IX)	1 st	1	0.9900	338	0.3	-2.5	-0.11	34.7
	2 nd	1	0.9661	619	0.2	-4.9	-0.11	63.15
$\text{Zn}_2(\text{H}_2\text{L}^2)\text{X}_2\cdot\text{H}_2\text{O}$ (X)	1 st	0.66	0.9994	313	3.4	0.8	-0.11	35.2
	2 nd	0.66	0.9942	600	3.2	-1.79	-0.17	100.2

X=Ac₂O

finally form the representative metal oxide. This may be attributed to the structural rigidity of the chelating ligands which requires more energy for its rearrangement to get the correct order compared with the activated complex [5].

- The activation energy E^* values calculated by the Coats–Redfern method are shown to follow the order Mn(II)>Co(II)>Zn(II)>Cu(II)>Ni(II) for the SADH and follow the order Co(II)>Zn(II)>Mn(II)>Cu(II)>Ni(II) for the DHBADH which is not perfectly in agreement with the electropositive character of the metal ions. The activation energy increases with increasing the ionic radius, thus confirming that the stability of the complexes of the ligands increases with the ionic radius. This discrepancy in the trend can be explained by the presence of the free OH group on the benzene ring of the metal complexes with the ligand DHBADH which occupies the meta-position on the azomethine group and may cause an induced strong electron delocalization over the whole metal complex. This high induced electron delocalization is of major contribution to the strength of the metal-ligand bonding and hence affects the stability of the complex. As the ionic radius of the metal ion increases, the delocalization along the azomethine group increases and the stability of the complex increases in the same direction.

The data of thermal analysis curves and the calculated activation kinetic parameters of the decomposition of the prepared complexes show that the thermal stability of metal complexes depends essentially on the nature of both the central metal ion and the ligand.

Conclusions

The foregoing results and discussion indicate that the thermal degradation of the metal complexes under study proceeds in four steps. The first is the dehydration of the complexes followed by the elimination of the acetate anions. The anhydrous anion-free complexes undergo decomposition to the metal oxide (MO) through the loss of the aldehyde part followed by the adipic dihydrazide portion in the fourth step. The third and the fourth steps intermingle together in most cases. The energy of activation of the thermal decomposition as determined from the rate of the reaction depends on the nature of the metal ions being in the order Mn(II)>Co(II)>Zn(II)>Cu(II)>Ni(II) for L¹ (SADH) and Co(II)>Zn(II)>Mn(II)>Cu(II)>Ni(II) for L². Also, the complexes of L² are more stable than those of L¹.

References

- J. H. Eapason and G. W. Kirker, Inorg. Chim. Acta, 40 (1980) 105.
- S. C. Bhatia, J. M. Bindlish, A. R. Saini and P. C. Jain, J. Chem. Soc. Dalton Trans., (1981) 1773.
- M. A. El-Ries, S. M. Abu-El-Wafa and S. M. El-Kosy, J. Pharm. Belg., 43 (1988) 93.
- R. M. Issa, S. M. Abu-El-Wafa and F. A. El-Sayed, Thermochim. Acta, 126 (1988) 235.
- S. S. Kandil, F. I. Abdel-Hay and R. M. Issa, J. Therm. Anal. Cal., 63 (2001) 173.
- N. A. El-Wakiel, J. Therm. Anal. Cal., 77 (2004) 839.
- E. Jóna, A. Maslejova, M. Kubranuva and P. Šimon, J. Thermal Anal., 46 (1996) 129.
- F. Kovanda, J. Therm. Anal. Cal., 71 (2003) 727.
- V. A. Logvinenko, E. A. Ukraintseva, D. V. Soldatov and T. A. Chingina, J. Therm. Anal. Cal., 75 (2004) 337.

- 10 W. Nowak, *J. Therm. Anal. Cal.*, 77 (2004) 125.
 11 S. M. Dakka, *J. Therm. Anal. Cal.*, 74 (2003) 729.
 12 R. M. Issa, S. M. Abu-El-Wafa, G. B. El-Hefnawy and N. El-Wakiel, *Egypt. J. Chem.*, 44 (2001) 99.
 13 A. I. Abdel-Monsef, 'Study The Preparation, Characterization and Toxicology of New Heterocyclic Nitrogen, Schiff Bases, Hydrazones and Their Metal Chelates' Ph.D. Chem. Dept. Tanta Univ., (2005).
 14 L. Meites, 'Polarographic Techniques' Interscience Publishers Inc., 1st Ed., NY 1955.
 15 K. Nakamoto, 'Infrared and Raman Spectra of Inorganic and Coordination Compounds', 3rd Ed., John Wiley, (1978).
 16 G. B. Deacon and R. J. Phillips, *Coord. Chem. Rev.*, 33 (1980) 227.
 17 R. Srinivasan, I. Sougandi, K. Velavan, R. Venkatesan, V. Babu and P. S. Rao, *Polyhedron*, 23 (2004) 1115.
 18 A. W. Coats and J. P. Redfern, *Nature*, 201 (1964) 68.
 19 A. S. A. Zidan, A. I. El-Sayed, M. S. El-Meleigy
 A. A. Aly and O. F. Mohammed, *J. Therm. Anal. Cal.*, 62 (2000) 665.
 20 A. A. Frost and R. G. Pearson, 'Kinetic and Mechanism', Wiley, New York 1961.
 21 R. M. Issa, A. M. Khedr and A. Tawfik,
 Synth. React. Inorg. Met-Org. Chem., 34 (2004) 1187.
 22 M. Greisher, J. Lewis and R.C. Slade, *J. Chem. Soc. A*, (1964) 1442.

Received: June 12, 2006

Accepted: July 27, 2006

OnlineFirst: February 26, 2007

DOI: 10.1007/s10973-006-7730-z